Electronic Supplementary Material (ESI) for Chemical Science.

Helical amplification system composed of artificial nucleic acids

Hiromu Kashida*, Keiji Nishikawa, Wenjing Shi, Toshiki Miyagawa, Hayato Yamashita, Masayuki Abe, Hiroyuki Asanuma*

kashida@chembio.nagoya-u.ac.jp (H.K.); asanuma@chembio.nagoya-u.ac.jp (H.A.)

Table of Contents

Materials and Methods

Oligonucleotides

SNA, D-*a*TNA, and L-*a*TNA monomers T, G, A, C were synthesized according to reported procedure.[1] The pyrene functionalized U was synthesized as described below. The oligomers were synthesized on an automated ABI-3400 DNA synthesizer (Applied Biosystems) using standard phosphoramidite chemistry. Several SNA oligomers were obtained from Hokkaido System Science Co., Ltd. Amino lcaa CPG 500-Å supports (ChemGenes) tethering SNA, L-*a*TNA, or D-*a*TNA monomers were used as was used as solid supports for oligomer synthesis. The coupling efficiency of these monomers was as high as that of the conventional monomers as judged from the color of the released trityl cation. Oligomers were purified by reversed-phase HPLC and were characterized by MALDI-TOFMS (Autoflex, Bruker Daltonics).

The MALDI-TOFMS data for the D-*a*TNA, L-*a*TNA or SNA oligomers were as follows: **S1**: Obsd. 3119 (Calcd. for [**S1**+H^+]: 3119). **S2**: Obsd. 3235 (Calcd. for [**S2** +H^+]: 3235). **S2F**: Obsd. 3235 (Calcd. for [**S2F** +H^+]: 3235). **S2t**: Obsd. 3217 (Calcd. for [**S2t** +H^+]: 3217). **S2c**: Obsd. 3187 (Calcd. for [**S2c** +H^+]: 3187). **S2gap**: Obsd. 2546 (Calcd. for [**S2gap** +H^+]: 2547). **DT1**: Obsd. 3259 (Calcd. for [**DT1** +H^+]: 3259). **LT1**: Obsd. 3259 (Calcd. for [**LT1** +H^+]: 3259). **S3**: Obsd. 2510 (Calcd. for [**S3** +H^+]: 2511). **S4**: Obsd. 2547 (Calcd. for [**S4** +H^+]: 2547). **DT3**: Obsd. 2623 (Calcd. for [**DT3**+H^+]: 2623). **S5**: Obsd. 1872 (Calcd. for [**S5** +H^+]: 1872). **S6**: Obsd. 1890 (Calcd. for [**S6**+H^+]: 1890). **DT5**: Obsd. 1957 (Calcd. for [**DT5** +H^+]: 1957).

Melting temperature measurements

Melting temperatures were determined by using a Shimadzu UV-1800. The melting curves were obtained by monitoring absorbance at 260 nm versus temperature. Both cooling and heating curves were measured and temperature ramp was 0.5 ºC min^{-1}. The sample solutions contained, unless otherwise noted, 10 mM phosphate buffer (pH 7.0), 100 mM NaCl, and 4.0 µM SNA, D-*a*TNA, or L-*a*TNA.

Thermodynamic parameters of duplex were determined from $1/T_m$ versus $\ln(C_t/4)$ plots by the following equation:

$$\frac{1}{T_m} = \frac{R}{\Delta H}\ln\left(\frac{C_t}{4}\right) + \frac{\Delta S}{\Delta H}$$

where C_t is the total concentration of nucleic acid, and $\Delta G°_{37}$ or $\Delta G°_{20}$ was calculated from ΔH and ΔS values.

Size-exclusion chromatography measurements

Size-exclusion chromatography was performed using a HPLC system equipped with a TSK-gel G2000SW (Tosoh) at 25 ºC. The buffer was 10 mM phosphate (pH 7.0), 100 mM NaCl, and the flow rate was 1.0 ml min^{-1}. The elution of oligomers was monitored by measuring the absorbance at 260 nm. Before measurement, the SNA sample was heated at 80 ºC for 3 min, then slowly cooled down to 0 ºC.

Circular dichroism (CD) measurements

CD spectra were measured on a JASCO model J-820 equipped with programmed temperature controllers using 10-mm quartz cells. Sample solutions containing oligomers were heated at 80 ºC for 3 min, then slowly cooled down to 0 ºC at a rate of 3.0 ºC min^{-1}. Spectra were measured at 20 ºC intervals. Each spectrum was measured after annealing unless otherwise noted. The CD intensity, ΔCD, was calculated by subtracting minimam intensity from maximum intensity of the couplet (see Fig. 2a). The sample solutions contained 10 mM phosphate buffer (pH 7.0), 100 mM NaCl, and 4.0 µM SNA, D-*a*TNA, L-*a*TNA, and indicated equivalents of the chiral strand, unless otherwise noted.

Atomic force microscopy (AFM) measurements

AFM measurements were performed with a laboratory-built high speed AFM (HS-AFM) apparatus similar to a previously reported AFM [2]. The detailed procedures towards HS-AFM imaging are reported elsewhere [3]. The HS-AFM was equipped with small cantilevers (k = 0.1 – 0.2 N/m, f = 800 – 1200 kHz in water (Olympus)) and operated in tapping mode. The AFM styli were grown on each cantilever by

electron beam deposition. A sample stage made of quartz glass was placed on the z-scanner, and a 1.5-mm-diameter mica disk was glued onto the sample stage. For HS-AFM measurements of the SNA nano wire, a freshly cleaved mica surface was treated for 3 min with 0.1% 3-aminopropyltriethoxysilane (aminosilane) solution in water. After rinsing the surface with ultrapure water, a 2μL sample droplet of 0.1μM SNA nano wire was placed on the mica surface and incubated for 3 min. HS-AFM observation was performed under a solution containing 10 mM phosphate (pH 7.0) and 100mM NaCl at room temperature.

The length of each imaged SNA nano wire was analyzed using SPIP image analysis software (Image Metrology) and Igor Pro (WaveMetrics).

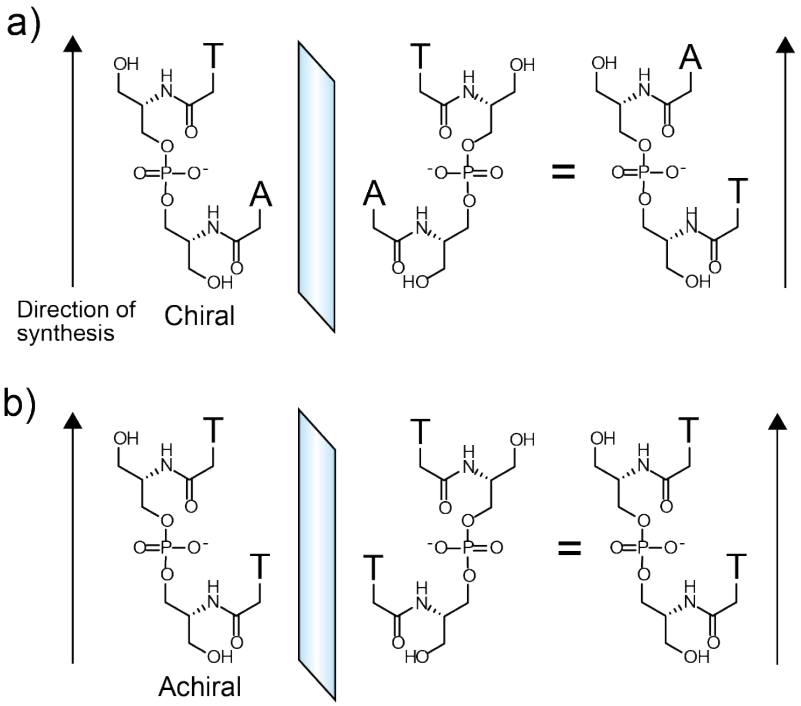

Figure S1. Control of chirality of SNA oligomers by sequence design. (a) The chirality can be reversed by inversing the sequence. (b) SNA with a symmetrical sequence is achiral (meso-form).

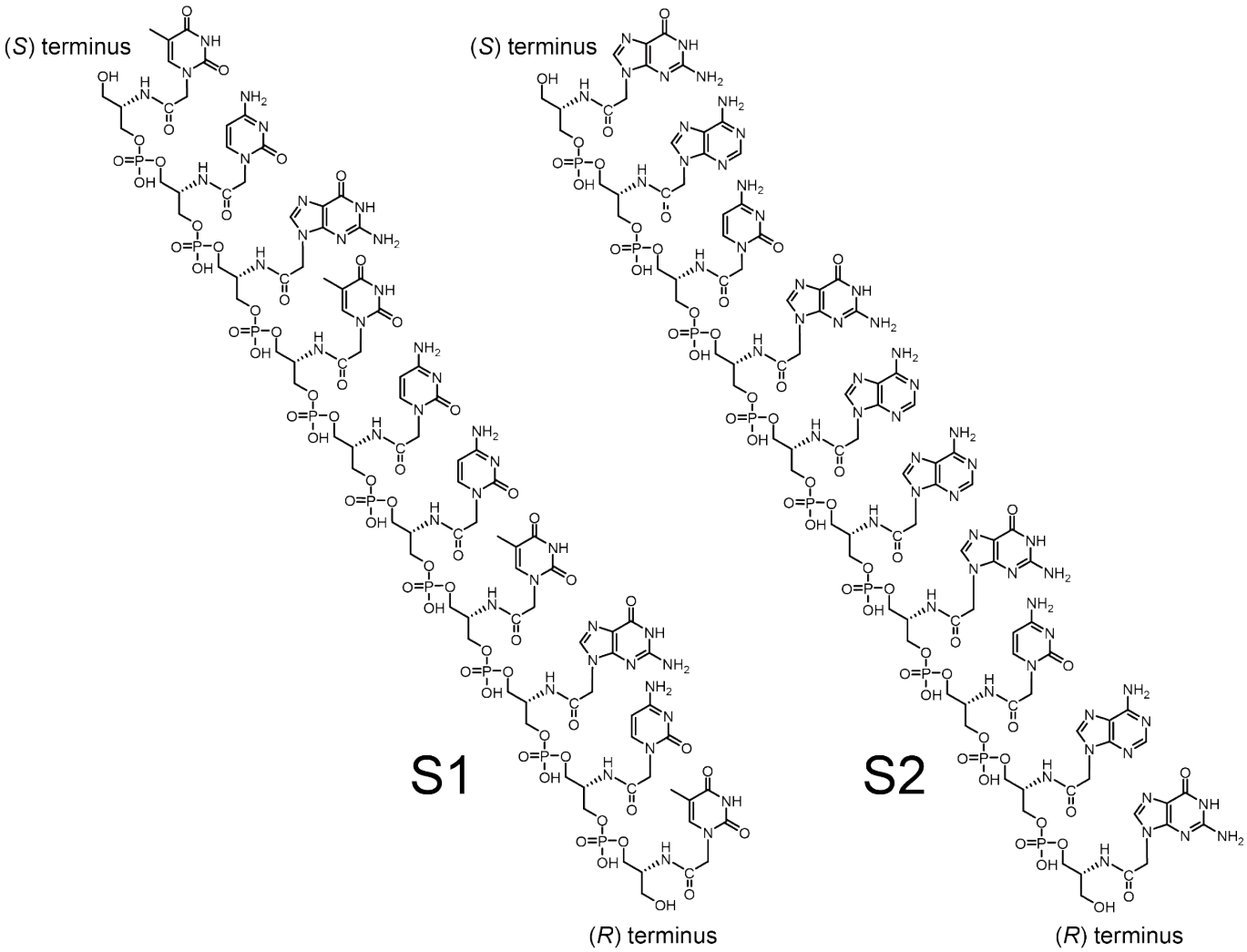

Figure S2. Chemical structures of S1 and S2. (*R*) and (*S*) termini are named according to the chirality of the terminal residues.

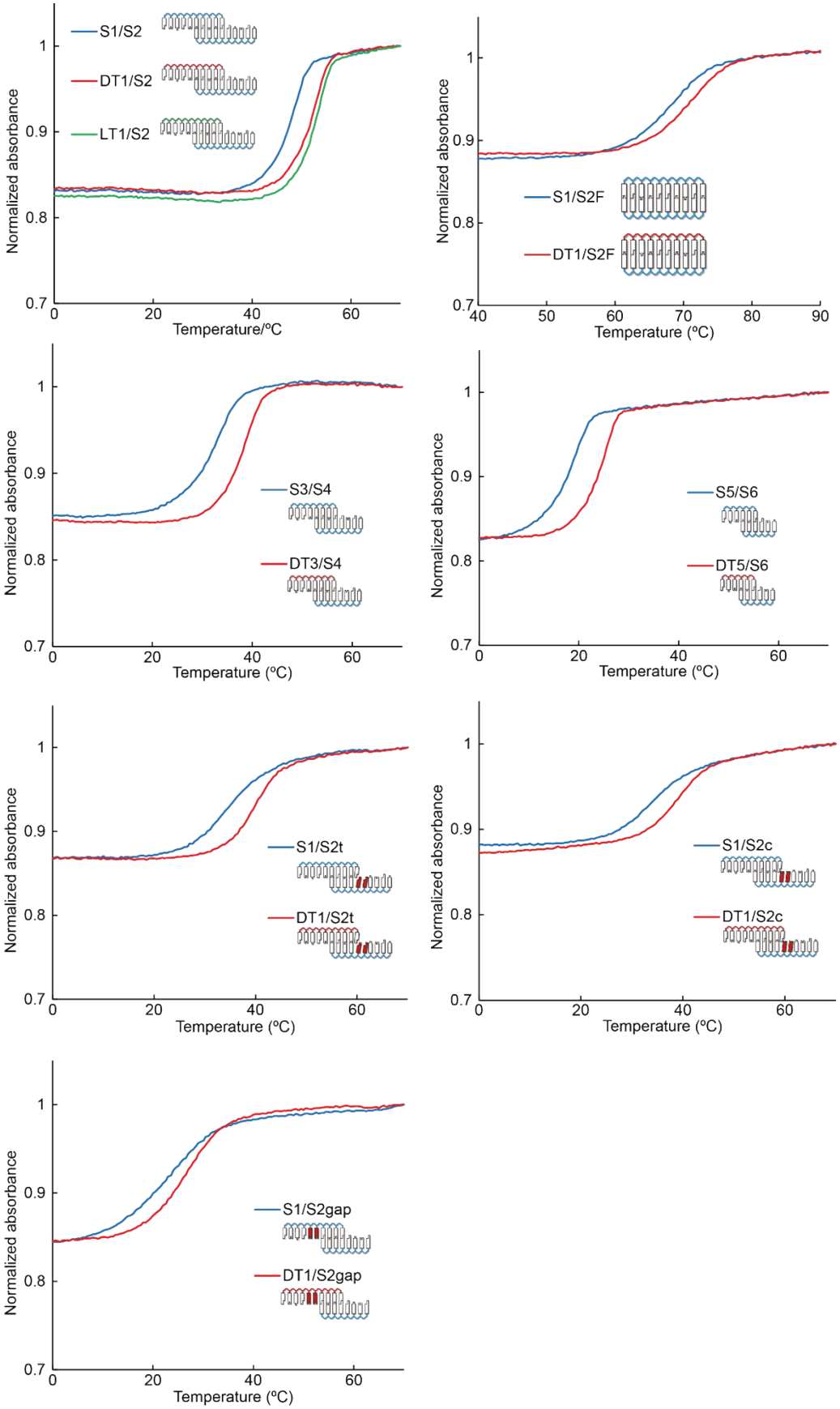

Figure S3. Melting curves of fully complementary duplexes and nanowires. Melting temperatures are listed in Table S1. Solution conditions were 4.0 μM each strand, 100 mM NaCl, 10 mM phosphate buffer (pH 7.0), 10 mm path length.

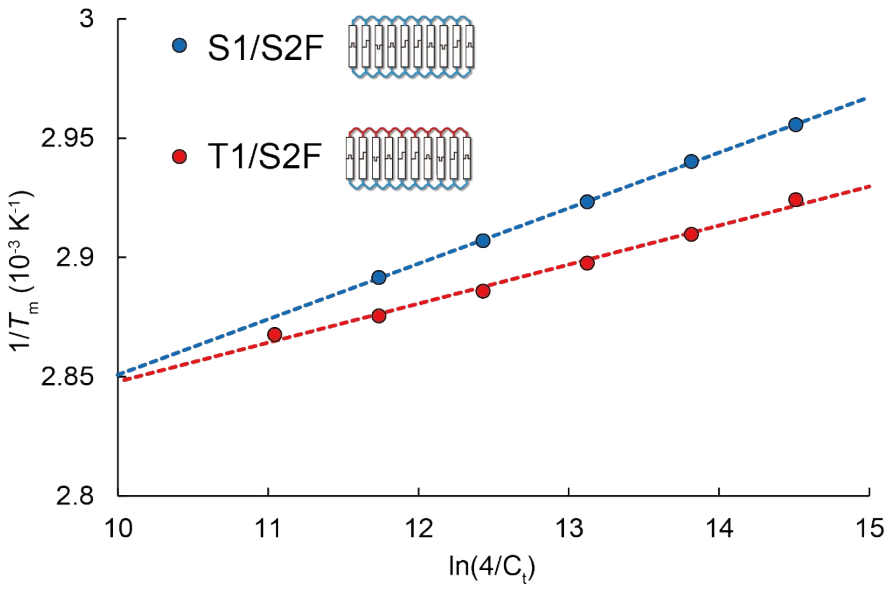

Figure S4. van't Hoff plots of SNA/SNA and D-*a*TNA/SNA duplexes. Solution conditions were 100 mM NaCl, 10 mM phosphate buffer (pH 7.0) 10 mm path length.

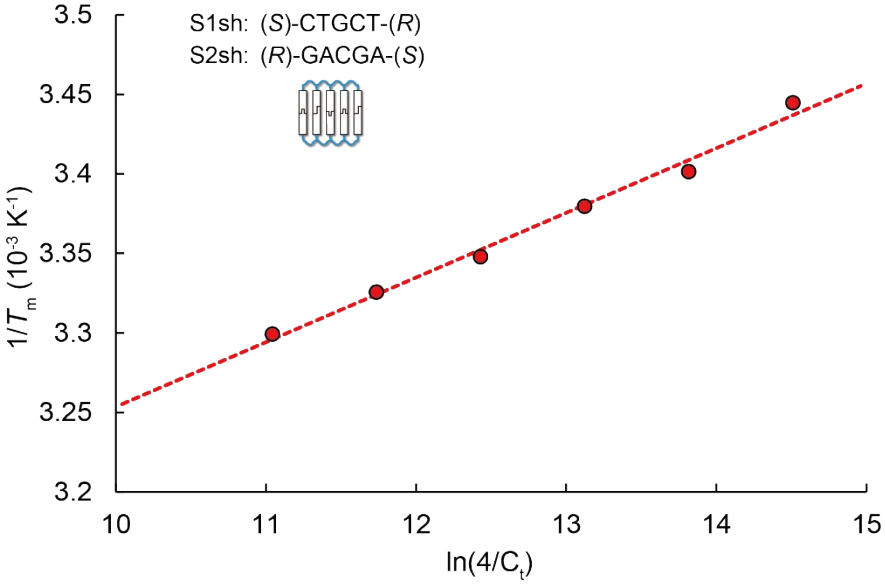

Figure S5. van't Hoff plot of S1sh/S2sh duplex. Sequences are also shown in the figure. Solution conditions were 100 mM NaCl, 10 mM phosphate buffer (pH 7.0) 10 mm path length.

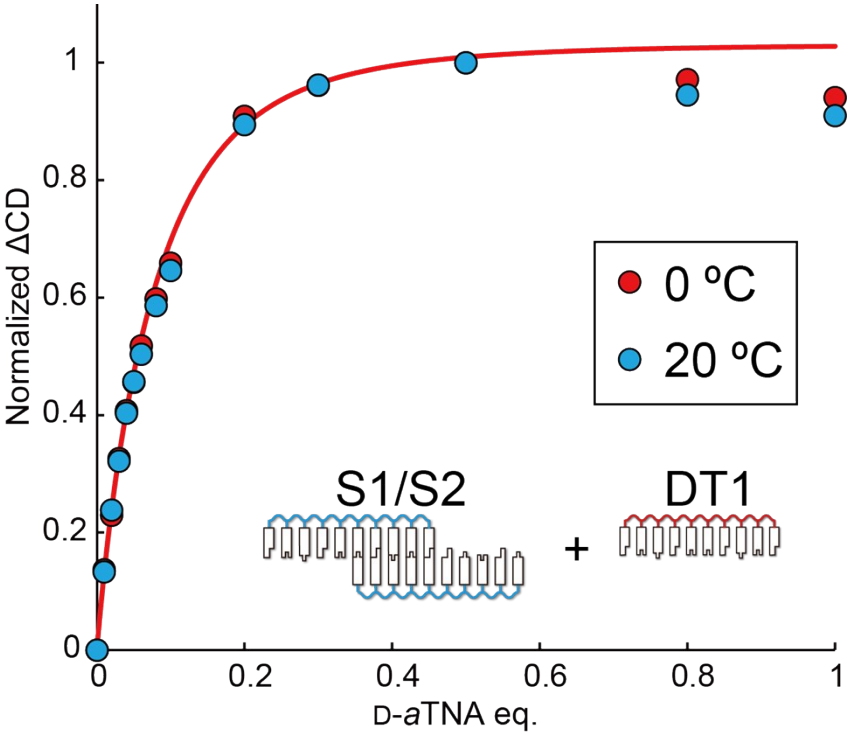

Figure S6. Effects of temperature on helical amplification. Plots of normalized ΔCD of S1/S2 versus number of equivalents of DT1 at 0 and 20 °C are shown. Solution conditions were 4.0 μM each SNA strand, 100 mM NaCl, 10 mM phosphate buffer (pH 7.0), 10 mm path length.

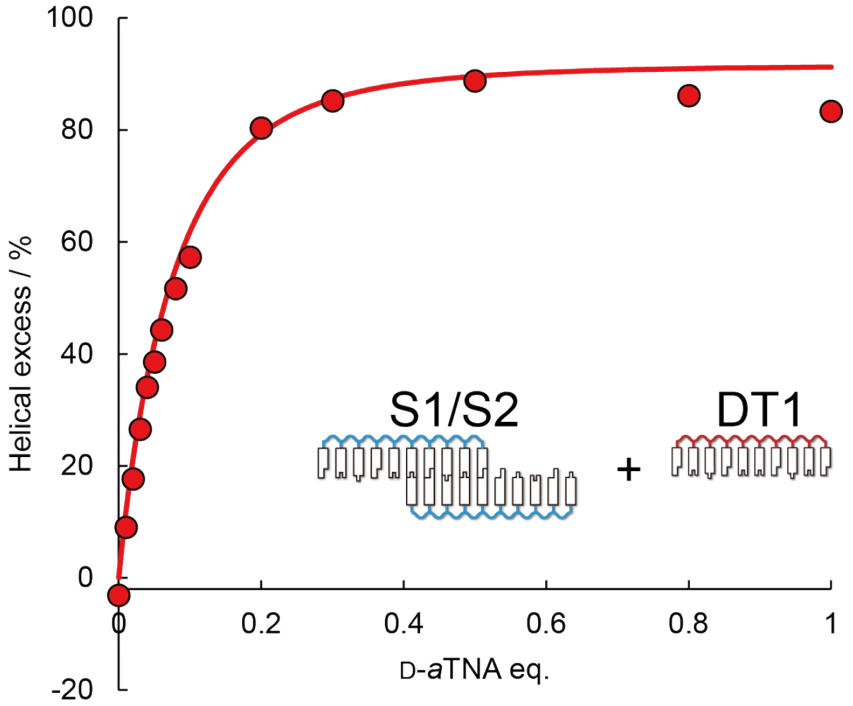

Figure S7. Plot of change in helical excess of S1/S2 versus number of equivalents of DT1. ΔCD value of DT1/S2 without S1 was used as a control with 100% helical excess. Solution conditions were 4.0 μM each SNA strand, 100 mM NaCl, 10 mM phosphate buffer (pH 7.0), 10 mm path length, 0 °C.

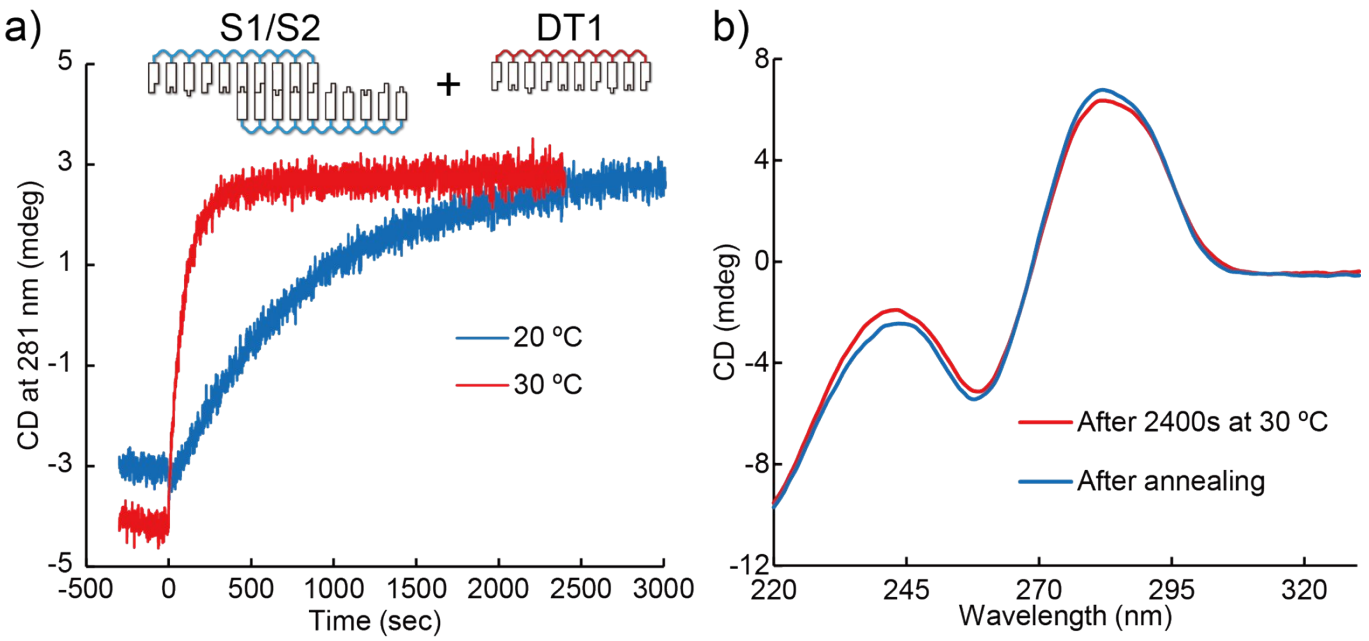

Figure S8. (a) Time course of change in CD of S1/S2 upon the addition of DT1 at 20 or 30 ºC (blue or red line, respectively). (b) CD spectrum of S1/S2 with DT1 after 60 min incubation at 30 ºC. CD spectrum of the same sample after annealing is also shown. Solution conditions were 2.0 μM each strand, 100 mM NaCl, 10 mM phosphate buffer (pH 7.0), 10 mm path length.

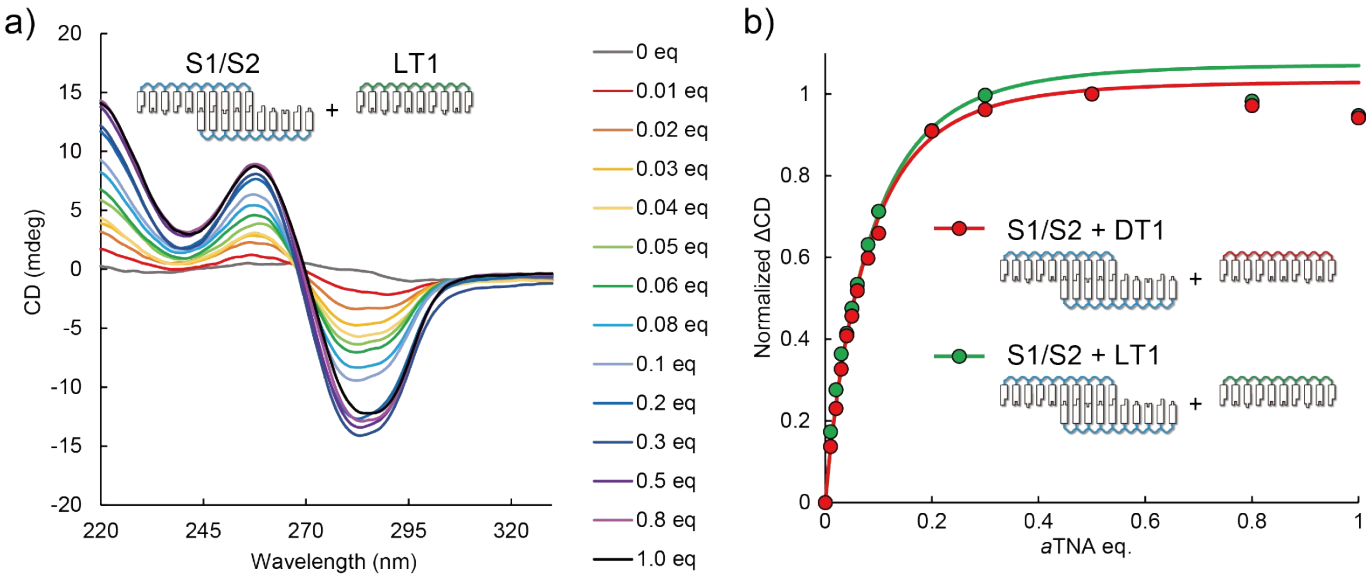

Figure S9. (a) CD spectra of S1/S2 with indicated numbers of equivalents of LT1. (b) Plots of ΔCD at 260 nm of S1/S2 versus number of equivalents of DT1 or LT1. Solution conditions were 4.0 μM each SNA strand, 100 mM NaCl, 10 mM phosphate buffer (pH 7.0), 10 mm path length, 0 °C.

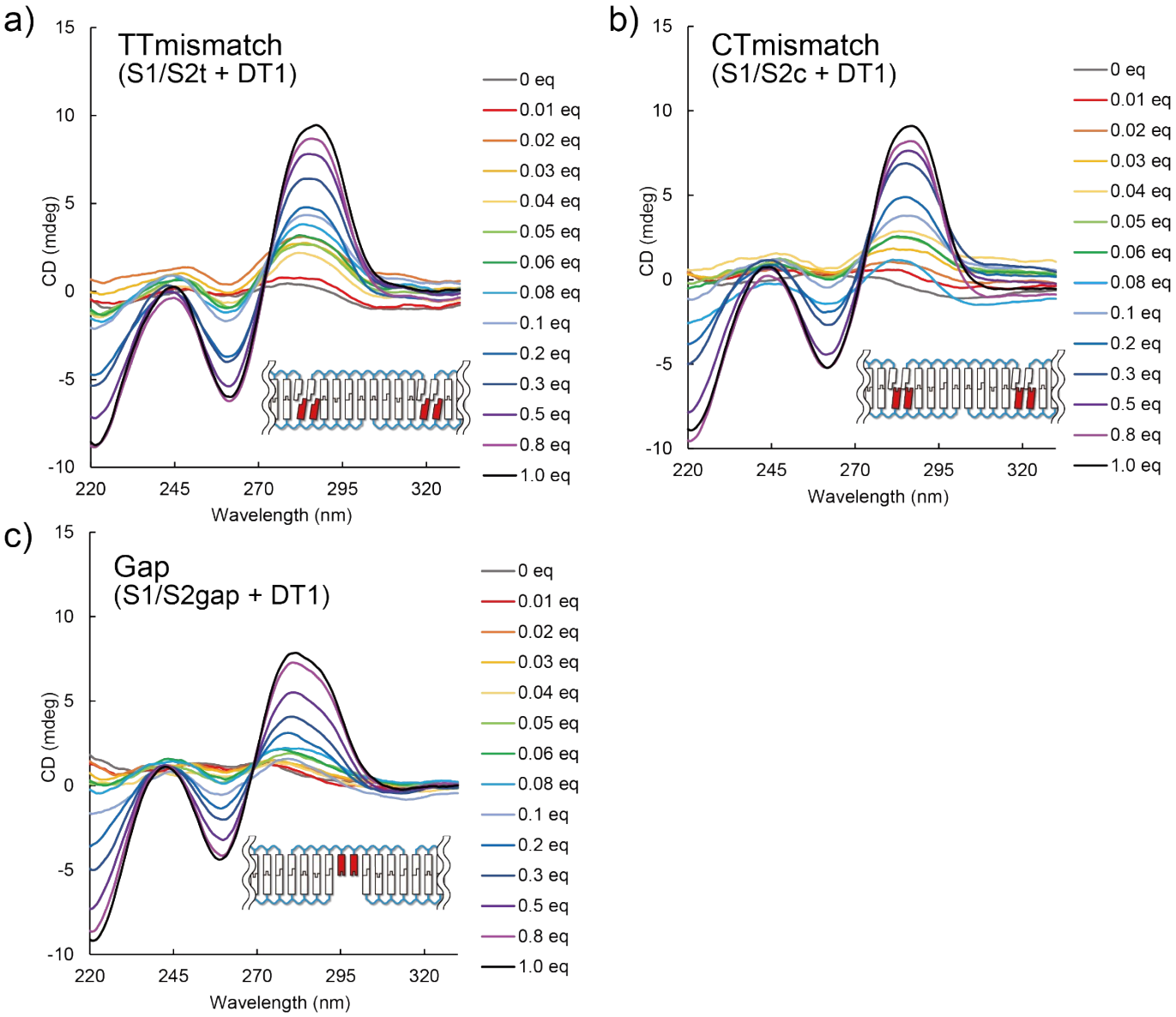

Figure S10. Effects of mismatches or gaps on helical amplification. CD spectra of (a) S1/S2t, (b) S1/S2c, and (c) S1/S2gap nanowires with indicated equivalents of DT1. Solution conditions were 4.0 μM each SNA strand, 100 mM NaCl, 10 mM phosphate buffer (pH 7.0), 10 mm path length, 0 °C.

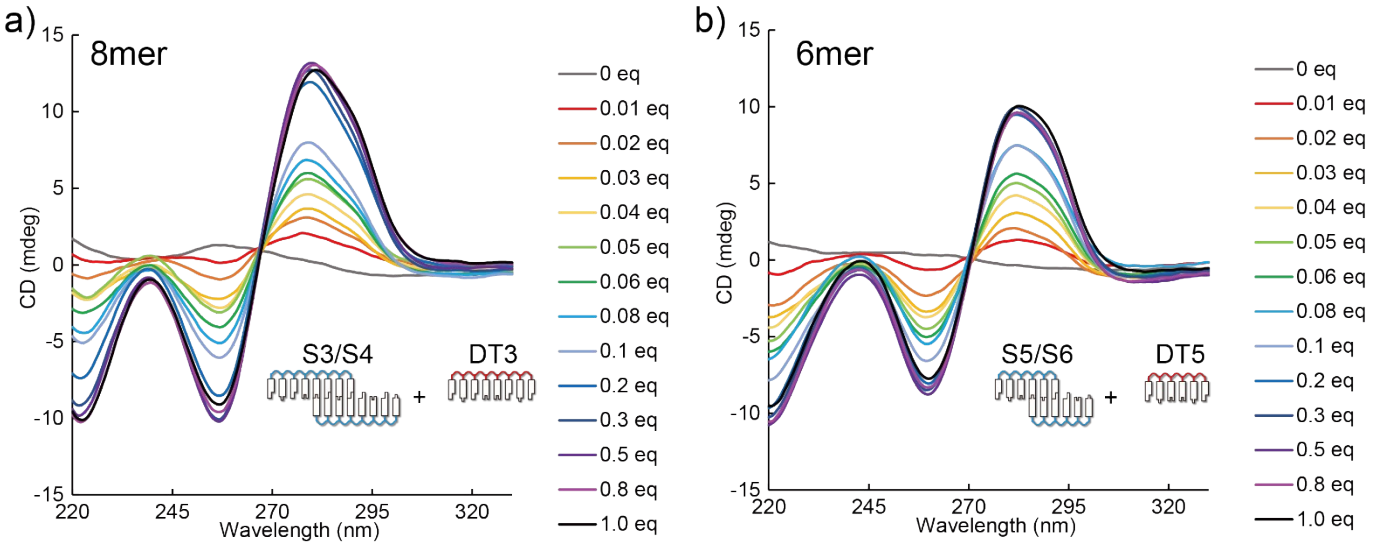

Figure S11. Effects of strand length on helical amplification. (a) CD spectra of S3/S4 nanowire with indicated equivalents of DT3. (b) CD spectra of S5/S6 nanowire with indicated equivalents of DT5. Solution conditions were 4.0 μM each SNA strand, 100 mM NaCl, 10 mM phosphate buffer (pH 7.0), 10 mm path length, 0 °C.

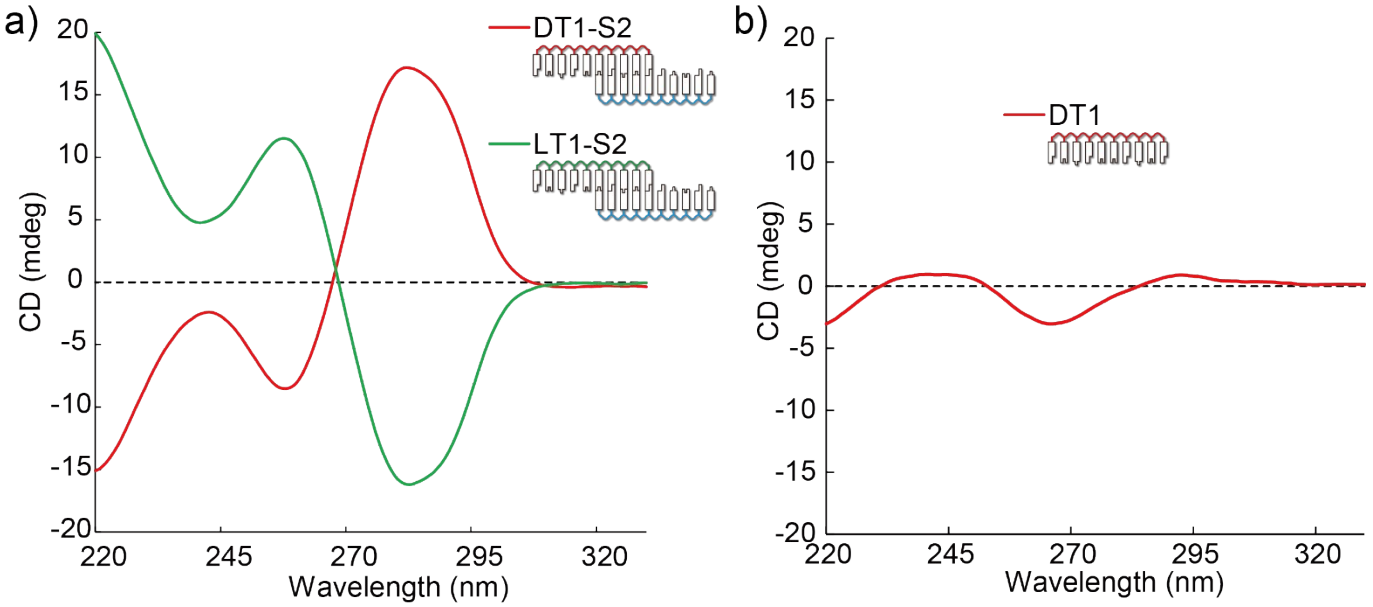

Figure S12. CD spectra of (a) DT1/S2 and LT1/S2 nanowires and (b) single-stranded DT1. Solution conditions were 4.0 μM each strand, 100 mM NaCl, 10 mM phosphate buffer (pH 7.0), 10 mm path length, 0 °C.

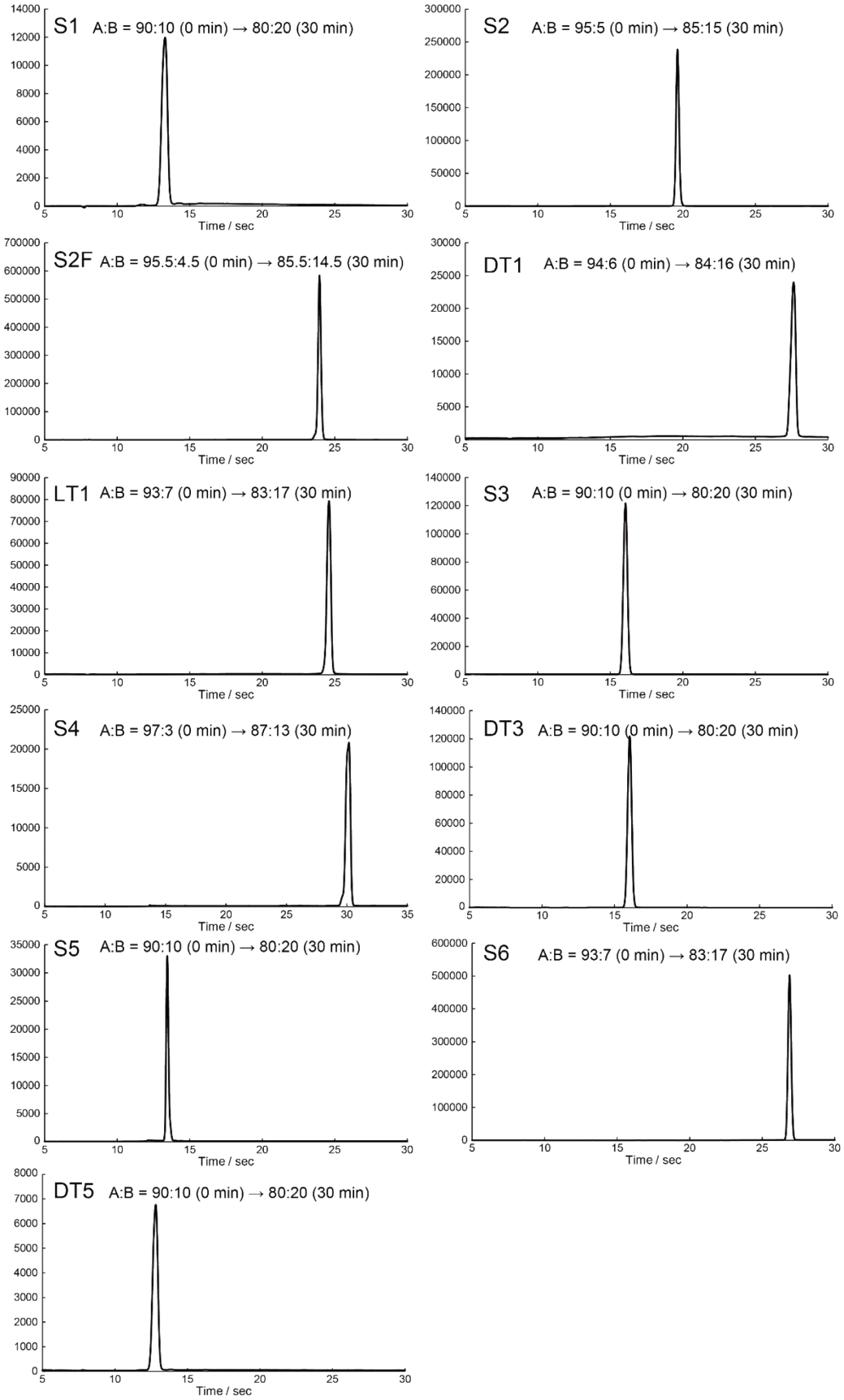

Figure S13. RP-HPLC chromatgrams of oligonucleotides. The flow rate was 0.5 mL/min. A solution of 50 mM ammonium formate (solution A), and a mixture of 50 mM ammonium formate and acetonitrile (50/50, v/v; solution B) were used as mobile phases.

Table S1. Melting temperatures of fully complementary duplexes and nanowires.

Name		Sequence ((*S*) or 1'→(*R*) or 3')		T_m (ºC)
S1/S2F (SNA/SNA)	S1	TCGTCCTGCT	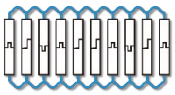	69.1
	S2F	AGCAGGACGA		
DT1/S2F (D-*a*TNA/SNA)	DT1	TCGTCCTGCT	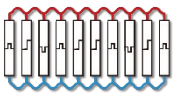	72.1
	S2F	AGCAGGACGA		
S1/S2 (SNA/SNA)	S1	TCGTCCTGCT	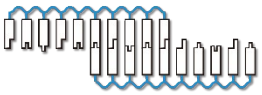	46.7
	S2	GACGAAGCAG		
DT1/S2 (D-*a*TNA/SNA)	DT1	TCGTCCTGCT	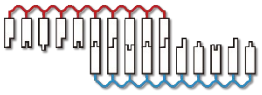	53.4
	S2	GACGAAGCAG		
LT1/S2 (L-*a*TNA/SNA)	LT1	TCGTCCTGCT	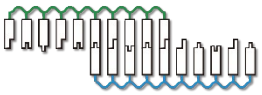	53.4
	S2	GACGAAGCAG		
S3/S4 (SNA/SNA)	S3	TGTCCTGT	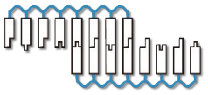	33.6
	S4	GACAACAG		
DT3/S4 (D-*a*TNA/SNA)	DT3	TGTCCTGT	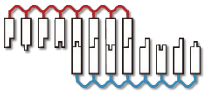	39.3
	S4	GACAACAG		
S5/S6 (SNA/SNA)	S5	TGCCGT	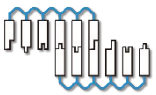	18.3
	S6	GCAACG		
DT5/S6 (D-*a*TNA /SNA)	S5	TGCCGT	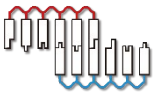	25.3
	S6	GCAACG		
S1/S2t (SNA/SNA)	S1	TCGTCCTGCT		33.8
	S2t	GACG**TT**GCAG		
DT1/S2t (D-*a*TNA/SNA)	DT1	TCGTCCTGCT		38.3
	S2t	GACG**TT**GCAG		
S1/S2c (SNA/SNA)	S1	TCGTCCTGCT		31.7
	S2c	GACG**CC**GCAG		

DT1/S2c (D-*a*TNA/SNA)	DT1 S2c	TCGTCCTGCT GACG**C**CGCAG		38.4
S1/S2gap (SNA/SNA)	S1 S2gap	TCGTCCTGCT ACGAAGCA		24.0
DT1/S2gap (D-*a*TNA/SNA)	DT1 S2gap	TCGTCCTGCT ACGAAGCA	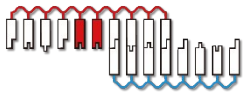	26.0
S1sh/S2sh (SNA/SNA)	S1sh S2sh	CTGCT AGCAG		22.9

Table S2. Thermodynamic parameters of SNA/SNA and SNA/D-*a*TNA fully complementary duplexes.

Duplex	−ΔH (kcal mol^{-1})	−ΔS (cal K^{-1} mol^{-1})	−ΔG°$_{37}$ (kcal mol^{-1})	K_a (M^{-1})[a]
S1/S2F	85.4	223.5	16.0	2.0×10^{11}
DT1/S2F	121.4	325.9	20.3	2.1×10^{14}

[a]Binding constants at 37 ºC

Table S3. Thermodynamic parameters of short SNA/SNA duplex.

Duplex	−ΔH (kcal mol^{-1})	−ΔS (cal K^{-1} mol^{-1})	−ΔG°$_{20}$ (kcal mol^{-1})	K_a (M^{-1})[a]
S1sh/S2sh	48.9	139.1	8.1	1.1×10^{6}

[a]Binding constant at 20 ºC

Supplementary References

1. (a) H. Asanuma, T. Toda, K. Murayama, X. Liang and H. Kashida, *J. Am. Chem. Soc.*, 2010, **132**, 14702-14703; (b) H. Kashida, K. Murayama, T. Toda and H. Asanuma, *Angew. Chem. Int. Ed.*, 2011, **50**, 1285-1288; (c) K. Murayama, H. Kashida and H. Asanuma, *Chem. Commun.*, 2015, **51**, 6500-6503.
2. (a) H. Yamashita, K. Voïtchovsky, T. Uchihashi, S. A. Contera, J. F. Ryan and T. Ando, *J. Struct. Biol.*, 2009, **167**, 153-158; (b) H. Yamashita, K. Inoue, M. Shibata, T. Uchihashi, J. Sasaki, H. Kandori and T. Ando, *J. Struct. Biol.*, 2013, **184**, 2-11.
3. T. Uchihashi, N. Kodera and T. Ando, *Nat. Protoc.*, 2012, **7**, 1193.